



Performance of Nanocomposite Polysulfone-Polyaniline Substrates for Enhanced Thin Film Membranes

Elsayed M. Elnaggar¹, Mohamed E.A. Ali², Mostafa M. Abo-Elfadl², Salah F. Abdellah³, Ehab S. Gad^{1,3}, Amr A. Sammak⁴, Gamal M. El-kady¹

¹Chemistry Dept., Faculty of Science, Al-Azhar University, Nasr City, Cairo, Egypt

²Egypt Desalination Research Center, of Excellence, Desert Research Center, Cairo, Egypt

³Department of Chemistry, Faculty of Science and Arts, Al-Jouf University, Sakaka, Saudi Arabia

⁴Chemical warfare administration, Egyptian Ministry of Defense, Cairo, Egypt

Abstract

Membranes fouling and their degradation using free chlorine are the most common challenges in the desalination process. A blend nano-composite polysulfone / polyaniline were prepared as a substrate for the active polyamide layer. In this work, nano polyaniline emeraldine salt was prepared using a simple chemical oxidative polymerization method. It was added to the polysulfone (PS) substrate layer in the presence of sodium lauryl sulfate as a hydrophilic agent to enhance reverse osmosis properties of the thin film composite membrane. Unmodified and modified polyaniline nano-particles membranes were characterized using XRD, EDX, FT-IR, SEM, particle size distribution and contact angle. The membranes performance was evaluated in terms of water flux and salt rejection using a cross-flow filtration unit. The results showed that the nano-composite membrane had much better water permeability (66 L/m²/h) compared to the control membrane (57 L/m²/h) without significant change in the percentage of salt rejection. The resistance of membranes to bio-fouling and chlorine degradation was evaluated using bovine serum albumin (BSA) as fouling model and sodium hypochlorite, respectively. The modified membrane was more resistant to bio-fouling and chlorine attack because of the strong electrostatic repulsion between poly-aniline PANI and BSA. The prepared polysulfone - polyaniline nano-composite substrate has been enhanced the performance of thin film composite as a reverse osmosis membrane.

Keywords: Thin film composite membranes; Polyaniline; Polysulfone; Fouling; Chlorination, sodium lauryl sulfate and Reverse osmosis membrane.

Introduction

Desalination is one of the main technologies to provide consumable water from brackish or saline water [1]. Reverse osmosis membrane technology (RO) is one of the most important choices of water desalination technology is, it shares up to 60% of the total world desalination capacity [2]. The most common membranes for desalination are thin-film composite (TFC) membranes [3]. Bio-fouling and chlorine tolerance is the most important common problems affecting membranes performance [4,5]. Polysaccharides, bovine serum albumin (BSA), proteins, nucleic acids, and humic acids are the main causes of organic fouling. Therefore, membranes modification with different nano-materials either in the substrate or in the active layer was studied. PANI has special characteristics, such as its ease of synthesis, environmental stability [6], simple doping/ de-doping chemistry, relatively low cost [7]. It has some applications in membrane technology, because

of the high surface energy and high hydro-philicity, it has been used for fabrication of super-hydrophilic membranes and super-hydrophilic surfaces and to increase the permeability of the membrane that due to increasing membrane porosity [8]. During membrane formation, PANI nano-particles were blended with the PS matrix polymer. In addition, incorporation of PANI in the membrane matrix can protect it against degradation because of its ability to act as a radical scavenger [9]. Recent studies of dispersing of PANI hydro-philicity and permeability of the membrane [10]. Other search used PANI in emeraldine base to synthesis PS/PANI ultra-filtration membrane that has pore-structure and high permeability and more hydrophilic blended membrane than PS membrane [11]. In addition, PANI was used to improve the water flux and salt rejection of poly-ethersulfone membranes, All the PS/PANI emeraldine base membranes had higher porosity, larger surface pore size, more vertically interconnected finger-like pores

*Corresponding author e-mail: salah15eg@yahoo.com (Salah F Abdellah Ali)

Receive Date: 28 January 2021, Revise Date: 21 February 2021, Accept Date: 23 January 2022

DOI: 10.21608/EJCHEM.2022.60278.3290

©2022 National Information and Documentation Center (NIDOC)

and fewer macro voids than PS membrane [12]. In this study, hydrophilic and conducting poly-aniline (PANI) nano-particles were used as a modifier to enhance the antifouling and chlorine resistance of TFC membranes. Membrane surface chemical composition, surface hydro-philicity, and morphology were characterized by X-ray (XRD) analysis, water contact angle measurement and scanning electron microscope (SEM), respectively. Pure water flux of the membranes was tested to reflect permeability of the membrane. Bovine Serum Albumin (BSA) and sodium hypochlorite were used to estimate the effect of PANI on the membrane properties against fouling and chlorine degradation respectively.

Experimental

Materials

Aniline monomer (molecular weight 93 g/mol, alpha chemica company India), sodium lauryl sulfate (SLS, adwic), ammonium peroxydisulfate (APS, rankem company), hydrochloric acid (37 % SDFCL fine chem.), acetone, methanol (Fisher chemical). Polysulfone (PS Udel P 3500 LCD MB7, MW= 77000 to 83000 g/mol., Solvay), non-woven polyester fabric (Vontron Membrane Technology Co.), 1,3,5-benzenetricarbonyltrichloride, (TMC), N,N-dimethyl formamid (DMF, Aldrich), n-hexane (TEDIA), m-phenylenediamine (MPD, >99%, ACROS), camphor sulfuric acid (CSA, ACROS), sodium chloride (EMD Chemical), Bovine serum albumin supplied by Sigma-Aldrich was used as a model foulant in membrane fouling experiments, sodium hypochlorite (NaOCl concentration of 12%, Alfa Aesar) were used as received.

Preparation of polyaniline nano-particles (PANI)

PANI nano-particles were prepared through the chemical oxidative polymerization of aniline in aqueous HCl by using micellar solutions polymerization method [13]. In brief, 0.49 g (0.0021mol) of APS was dissolved in 10 ml of 0.1 M HCl solution and then added drop-wise into 100 ml of aqueous solution of aniline (0.43 g / mol) and SLS (0,034 g / mol) at 1.0 ml/min. The molar ratio of aniline to APS was kept at 2:1 through the entire experiment, and the total volume of the mixture after the addition of the initiator was raised to 110 ml. The polymerization was performed at $25 \pm 0.1^\circ\text{C}$ with a mechanical stirrer at 500 rpm in a two-neck round-bottomed flask mounted in a thermostat for 12 h. An excess amount of methanol was added to the HCl-doped PANI dispersion in order to precipitate PANI powder by breaking the hydrophilic-lipophilic balance (HLB) of the system and to stop the reaction. The precipitates were collected using a glass filter, then washed at least two times each with methanol, acetone, and distilled water to remove the unreacted chemicals such as aniline monomers and SLS. Then,

the PANI nanoparticles (emeraldine salt) were dried in the absence of moisture. We select this method after preparing PANI by other two different methods and comparing the yield particle size. The obtained results showed that this method gives the smallest nanoparticle size and highest yield.

Preparation of PS and PS/PANI support layer

PS and PS/PANI solutions were cast onto non-woven polyester fabric supported via the phase inversion process. The casting solution was prepared as follows; firstly, PANI was dispersed in DMF contains SLS with continuously stirring for 30 minutes, and then sonication for 30 minutes. After that, PS beads were added with continuous stirring at 90°C for 6 h. The concentration of PS was constant (16 %) for all casting solutions, whereas PANI was varied from 0 to 0.4 wt%. Table (1) shows the detailed preparation conditions of the casting solution at different concentrations of PANI. After complete dissolution of PS, all casting solutions were stored overnight at room temperature to release the air bubbles, the amount of SLS was determined as a result of complete dispersion of PANI by means of the amount of SLS tested for all PS/PANI concentrations solution to finally give completely dispersed PANI on PS solution with no precipitate. Then the solutions were cast onto non-woven polyester fabric with a casting knife to achieve a thickness of 200 μm . The phase inversion process occurred through immersion in a coagulation bath of distilled water. The non-woven fabric supported membranes were rinsed with de-ionized water to remove residual solvent.

Table (1): Composition of the casting solutions

Membrane	PS Conc. (W/w %)	PANI Conc. (W/w %)	SLS Conc. (W/w %)
PS	16	0	0
PS/PANI _{0.05}	16	0.025	0.1
PS/PANI _{0.05}	16	0.05	0.2
PS/PANI _{0.1}	16	0.1	0.3
PS/PANI _{0.2}	16	0.2	0.4
PS/PANI _{0.4}	16	0.4	0.5

Preparation of the polyamide active layer

The polyamide active layer was deposited onto the surface of PS and PS/PANI substrates via interfacial polymerization process of MPD in the aqueous phase and TMC in organic phase [13]. Where the substrates were initially immersed in MPD aqueous solution (2 % w/v) containing 1% CSA and 0.2 SLS as additives for two minutes, the excess solution was removed using a soft rubber roller. Then the amine saturated substrate was instantly submerged in 0.1% TMC contained in hexane solution for 60 sec. Thereafter, the resulting membrane was wiped at 80°C for 5 min, and

finally washed thoroughly and kept in deionized water.

Characterization

To confirm the polymerization of aniline to PANI nanoparticles, X-ray diffraction (X-ray diffractometer model X Pert pro diffractometer, Netherland), Scanning Electron Microscopy (Quanta FEG250 SEM, FEI Company), EDX (FEI-inspects model), FT-IR (model: M-IR-ASER CLASS1 WEEE-Reg NO DE84716930 -24V; 3.0A, Germany) were used. Moreover; Particle Size distributions of PANI suspensions were determined using Particle Size distribution analyzer System (CW388-V1.71\Cw388.tbl, Santa Barbara Calif., USA). The prepared TFC membranes were characterized with FT-IR, SEM, EDX and contact angle analyzer (VCA Video Contact Angle System, KrÜss DSA25B, Germany) at room temperature.

Evaluation the Membrane performance for desalination

The desalination performance of the membranes for water was measured in term of water flux and salt rejection using a cross-flow permeation apparatus (laboratory DDS reverse osmosis system (Alfa Laval), model LAB-20, manufactured by the Danish Sugar Corp., LTD, Denmark, Fig. 1 [14]. It consisted of 20 membrane cells, and each cell had an effective membrane diameter area of 18 cm². This allowed 20 membranes to be measured under typical conditions. The applied operating conditions were pressure 10 bars, NaCl concentration in feed water 2000 mg/l, temperature 25 °C, and pH 7. During the reverse osmosis runs, the retentate solution was re-circulated to the feed tank, and the permeate samples from the membrane cells were also recycled back to the system upon measurements of their solute concentrations individually. The salt rejection (R_s) and water flux (J_w) in L/m².h were calculated using the following two equations, respectively;

$$R_s \% = 100 \times \left(1 - \frac{C_p}{C_f}\right) \quad (1)$$

$$J_w = \frac{Q}{A \times t} \quad (2)$$

Where C_p and C_f are the concentrations of salt in permeate and feed respectively. Q is the volume of the water permeates (in liter) collected over an interval time " t " for a membrane surface area of " A ". C_p and C_f were determined using an Orion.

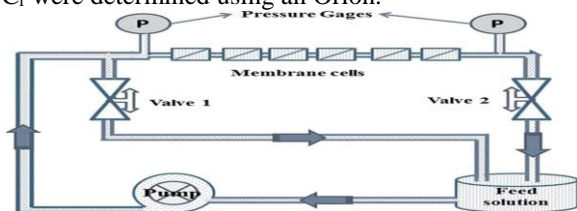


Fig. (1) Schematic diagram of the cross-flow unit used in this Study

Evaluation of membrane resistance to organic fouling

Membrane fouling was assessed by means of filtration-cleaning cycles. The feed saline solution contained 2000 mg/l of NaCl, and BSA was used as a model protein foulant. The experiment was conducted as follow; First, the membranes were activated by using distilled water for 1h, then the membrane preconditioned with a saline solution (2000 mg/l NaCl) at a pressure of 10 bar, and the initial water flux was determined when the water flux reached a steady state, the membranes were subjected to a filtration test with a saline solution of 2000 mg/l of NaCl containing 100 mg/l of BSA for another 6 h. After that, the membranes were rinsed thoroughly with deionized water for 2 h, Membrane fouling was evaluated through cross-flow filtration described above. The water permeate of each cell was collected separately for volume measurement, and then returned to the feed tank to keep the feed concentration approximately constant. The resultant flux profile was utilized to analyze the BSA fouling behavior of the tested membrane. In order to evaluate the membrane anti-fouling property, the flux recovery ratio (FRR) was calculated using Eq. (3) [15]:

$$FRR \% = (J_t / J_0) \times 100 \quad (3)$$

Evaluation of membranes resistance to chlorine

To evaluate the chlorine resistance of the membranes, the water flux, and salt rejection was measured with a feed saline solution (2000 mg/l NaCl) containing 600 mg/l of NaOCl at an applied pressure of 10 bar for an operation time of 6 h. The variations in water flux and salt rejection were monitored as permeation proceeded with time.

Results

Preparation and Characterization PANI Nanoparticles

Polyaniline was prepared using the chemical oxidative polymerization method using APS as an oxidant; this process is simple and fast with no need for special instruments. Through the reaction, the cation source (anilinium chloride precursor) was produced by the reaction of aniline monomer and hydrochloric acid, while APS acts as redox initiator. The two electron oxidation reaction of these two precursors led to the generation of aniline nitrenium (C_6H_5NH) cation that reacted with hydrochloric acid as dopant leading to the formation of dark green-colored PANI emeraldine salt nano-particles. The controlling of nano-particles formation was depend mainly on the rate of addition of APS oxidant that was constant at 1 ml/min at a constant speed of mechanical stirring of aniline solution (500 rpm) [16]. Fig. 2a shows the FT-IR spectrum of the prepared PANI, where the two characteristic peaks appeared at 1566 and 1483 cm⁻¹ correspond to the C=N stretching deformation of the

quinoid ring (Q) and C=C stretching deformation benzenoid rings of, respectively. In addition, the appeared peaks at 1291, 1235 and 995 cm^{-1} correspond to the stretching of secondary aromatic amine and C–N⁺ stretching vibration in the polaron structure (amorphous lattice) of PANI and C–Cl group vibration, respectively [17]. The degree of crystallinity of the PANI was determined using XRD (Fig. 2b), where four diffraction sharp peaks of $2\theta = 9.3, 15.5, 20.9$ and 25.6 were appeared that indicates the efficient formation of semi-crystalline conductive nano-PANI. The peaks at 25.6 and 20.9 are confirming low crystallinity of the conductive polyaniline. Also, crystallinity index can be calculated according to the following equation:

$$\text{Crystallinity} = \frac{\text{Area of crystalline peaks}}{\text{Area of all peaks}} \times 100 \quad (4)$$

Moreover, the appeared peak at $2\theta = 25.6$ represents the characteristic distance between the ring planes of benzene rings in adjacent chains or the close contact interchange distance [18]. SEM image (Fig. 2c) shows granular particles morphology of PANI “structural directors” which was controlled through the polymerization method. The particle size distribution of PANI dispersed in water was analyzed by particle size distribution analyzer, Fig. 2d. It was found that the particle size ranged between 47 and 243 nm with a mean diameter of 145.7 nm. The elemental compositions obtained from EDX of the prepared PANI-ES reveals that the weight percent of C, N, O, S, and Cl were found to be 82.27, 9.02, 6.06, 0.25, and 2.39 wt. %, respectively Fig. 2e.

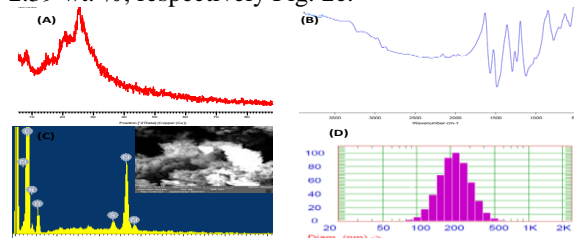


Fig. (2) characterization of prepared PANI nanoparticles, a) XRD patterns of PANI, b) FT-IR spectra of PANI, c) SEM and EDAX curve of PANI, d) particle size distribution analyzer of PANI

Characterization of PS/PANI membrane

FT-IR spectra of PANI, PS and PS/PANI membrane are shown in Fig. 3. Where, in the spectrum of PS, the characteristic peaks observed at 1584, 1492, 1307 and 1241 cm^{-1} are corresponding to benzene ring stretching, C–C stretching, C–SO₂–C symmetric stretching and C–O–C stretching respectively. All these peaks are close to that of PANI, which appeared at 1566, 1483, 1291 and 1235 cm^{-1} , therefore it is difficult to distinguish the change in the two spectrum

due to the low content of PANI in the casting solution (0.025 - 0.4) of PS weight. However; there are two new peaks, close to PANI nano-particle, was observed in the spectrum of PS/PANI at 1297 and 1014 cm^{-1} that corresponds to C–N stretching of secondary aromatic amine and C–Cl group vibration [19]. Fig. 4 shows the FT-IR spectra of the polyamide (PA) active layer deposited over the unmodified and modified substrates. Where in the two spectra, the observed peak at 1654 cm^{-1} , corresponding to the C=O stretch of the amide group, indicates successfully formation of the PA layer. The bands at 1735 cm^{-1} and 1450 cm^{-1} could be assigned to the characteristic peaks of C=O stretch and O–H deformation of the residual carboxylic acid groups, respectively. However; the appearance of the carboxylic acid functional groups was attributed to the hydrolysis of the un-reacted acyl chloride unit of TMC. In this work, the cross-linking degree of the PA layer formed over different substrates was also analyzed through the ratio of peak intensities. The characteristic peaks of 1735 cm^{-1} and 1450 cm^{-1} , which correspond to the carboxylic acid group were employed as the quantitative indication of acid content [20]. Where, with increasing PANI content in the substrates, the ratio of the peaks appeared at 1450 (–COOH)/1620 (–CON) and 1732 (–COOH)/1620 (–CON^{1/4}), it decreased to reach a minimum then increased. The acid content in the active layer of PA/PS/ PANI membranes had minimal value, indicating that the PA layer over PS/PANI-substrate possessed the highest cross-linking degree. It is well known that the interfacial polymerization occurs predominantly and if these acid chlorides can react with more m-phenylenediamine, the PA film would be denser and more cross-linked [18]. Fig.5 shows SEM images of the surface and cross-section of the unmodified and modified membranes with different concentrations of PANI. It is clear that the morphologies of the membrane surface of the control membrane show clearly a dense skin layer. Whereas, all PS/PANI modified membranes were shown to be more porous than PS membrane with spongy structure and from the surface images of membranes M2- M3- M4-M5 we can conclude that the micellar polymerization is not the best technique to prepare nano-composite hydrophilic PANI/PS membranes for UF and RO applications. In addition, the membrane porosity increased as PANI nano-particle ratio increased from 0.025% to 0.4% and had good interconnection, especially at low and high concentrations of PANI. These data confirmed that PANI was acted as a pore forming agent during membrane formation [21]. Cross section SEM images of the substrates show that all of the substrates have an asymmetric structure consisting of a dense top layer and a porous sublayer. The long finger-shaped pores were developed from the top to the bottom layer for all

membranes, in PS control membrane the Finger-like macrovoids were observed as narrow macrovoids, in modified PS/PANI membranes the finger-like macrovoids wear increased. Fig. 6 shows the quantitative analysis of PS and PS/PANI was investigated using EDX, wherein the PS membrane, the weight percentage of carbon, oxygen, and sulfur was 86.38%, 11.57%, and 2.06%, respectively. The addition of PANI nano-particle in PS substrate with different concentrations exhibited an ascendant and broadened ridge-valley structure, suggesting variation under different PANI nano-particle concentration there are an additional peaks beside main PS peaks such as Cl peak, and observed that the ratio percent of C, O was decreasing, and the ratio percent of S was increased as follow; C- 83.78 %, O- 11.43 %, S- 3.79 % and Cl- 0.40 % which indicates the incorporation of PANI in the composite matrix of membrane [12]. Contact angle analysis was used to evaluate the hydrophilicity of unmodified and modified substrate membranes. Fig.7 shows that contact angle values decreased from 74° for PS to 42° as PANI increased up to 0.05 %, then decreased with a high load of the nano-particle in the casting solution. This indicates that the inclusion of polyaniline in the casting solution was a useful way to enhance PS membrane hydro-philicity.

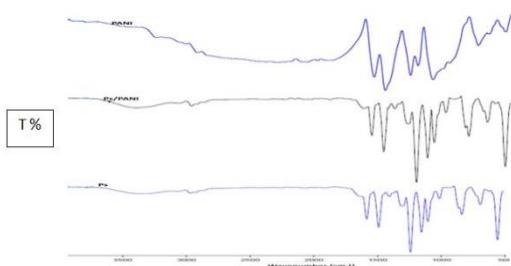


Fig. (3) FT-IR of PS, PS/PANI membranes (without thin film) and PANI nanoparticles

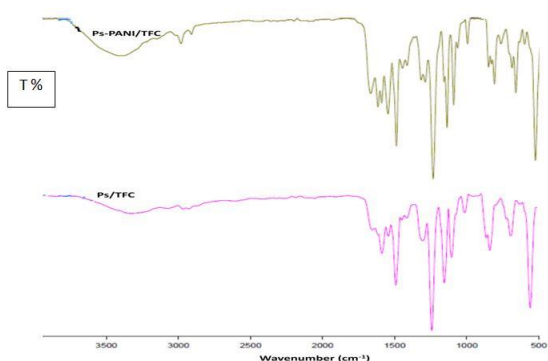


Fig.(4) FT-IR of PS membrane with TF and PS/PANI modified membrane wit TF

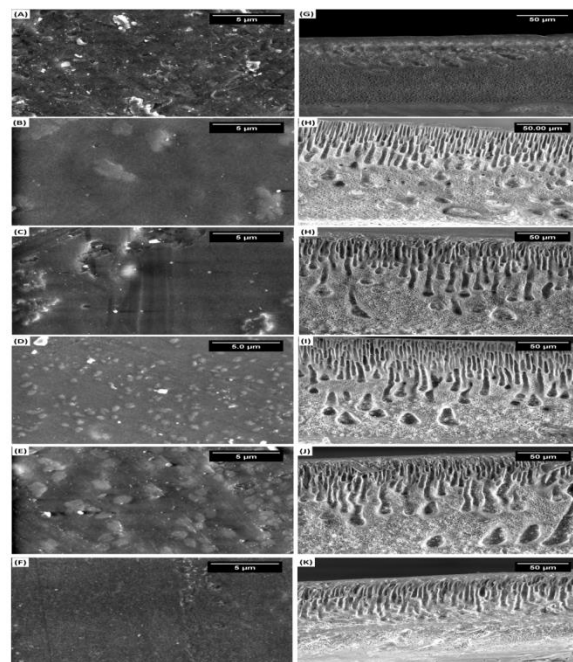


Fig. (5) SEM images of the top surfaces of membranes a) PS, b) PS/PANI (0.025), c) PS/ PANI (0.05) d) PS/PANI(0.1), e)PS/PANI(0.2),f)PS/PANI(0.4) and their cross sections of membranes G)PS, h) PS/PANI(0.025), I) PS/PANI(0.05), J) PS/PANI(0.1), K) PS/PANI(0.2), L) PS/PANI(0.4).

Desalination performance

The pure water permeation (PWP) of PS and PS/PANI membranes was conducted using DI water as feed solution at different applied pressures of 2, 4, and 6 bar at temperature. Fig. 8 shows that PWP of PS/PANI composite membranes with mass ratios of

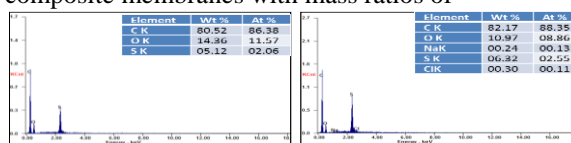


Fig. (6) EDX of membranes PS and PS/PANI.

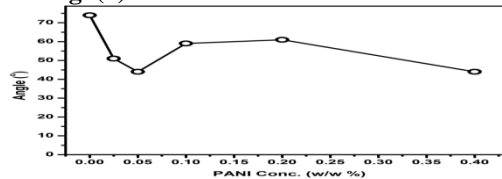


Fig. (7) Contact angle diagram of PS membrane and modified PS/PANI different concentration membranes.

0.025, 0.1 and 0.2 wt. %, was higher than PS membrane by 1.8, 1.8 and 1.7 times, respectively. In addition, the figure illustrated that PWP was increased with increasing from 2 to 6 bars for all membranes. This might be the composite membranes had superior hydrophilic characteristic because of the addition of PANI nano-particle that due to increased porosity and pore size of the substrate. The membranes

performance during desalination was examined using a synthetic solution NaCl with a concentration of 2000 mg/l at 10 bars as applied pressure. Fig.9 shows that both water flux and salt rejection increased as PANI nano-particles increase from 0.025 to 0.1 % then they were abruptly decreased. As PANI concentration increased more than 0.1 %, the membrane water flux was shown to be decreased, which might be related to block of pores of the membranes at high concentration of nano-particles [22]. These observations are shown in SEM and morphological results. Membrane salt

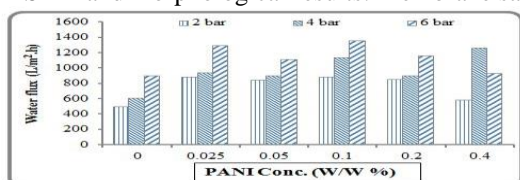


Fig. (8) Pure water permeation (PWP) of PS and PS/PANI different concentration membranes.

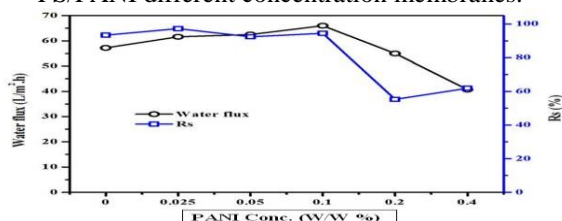


Fig. (9) Variation of NaCl solution flux and salt rejection of PS and PS/PANI different concentration membranes.

rejection was investigated by using of NaCl solution (2000) mg/l, Fig. 9. The results indicated that increase of PANI nano-particle concentration up to 0.1% wt in the PS casting solution led to decreasing of sodium chloride rejection of the prepared RO membranes. This probably due to the adsorption characteristic of PANI nano-particles, which caused preferable interactions between ions and the membrane matrix? The rejection was decreased by the increase of PANI nano-particle concentration from 0.1 to 0.4 % in the membrane matrix. This can be attributed to nano-particle agglomeration at the high additive concentration which decreases the amount of adsorptive active sites/active surface area, thereby decreasing salt adsorption capability by composite nano-particles, leading to increasing of ion percolation throughout the membrane [23].

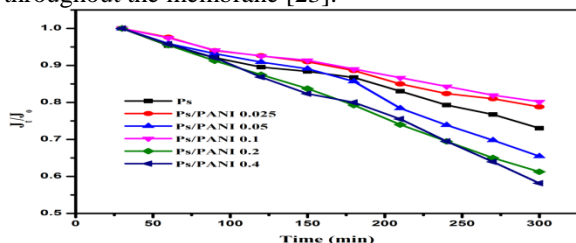


Fig. (10) Variation of BSA solution flux and salt rejection PS and PS/PANI different concentrations membranes

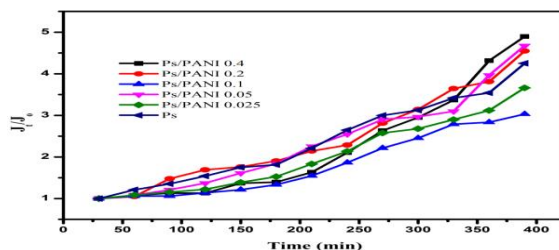


Fig.(11) Variation of (NaOCl) membrane decline curve of PS and PS/PANI membranes

Membrane fouling is an important issue that affects the separation performance of membranes and it is due to the flux decline of the membranes during the desalination process, in this section; BSA (100 mg/l) was used as a model foulant in feed solution containing 2000 mg/l of NaCl to illustrate the effect of PANI onto flux stability [24]. However, the flux decline was calculated by dividing the water flux at interval times (J_t) onto the initial water flux (J_0), Fig. 10. It can be seen that J_t/J_0 of the modified PS/PANI is lower than Ps membrane. In addition, because of PANI is a conductive polymer, it increased the surface hydro-philicity [25]. Membrane hypochlorite resistance was determined by means of changes in water flux for both PS and PS/PANI membranes after exposure to 600 mg/l of chlorine solution over a period of time (6.5 h). It is

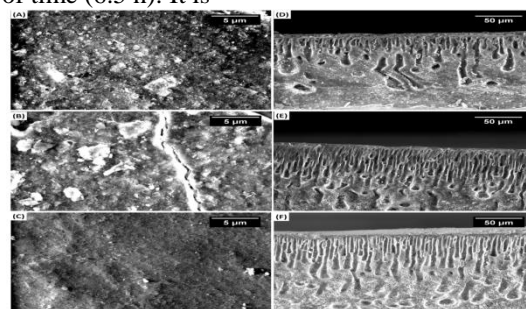


Fig.(12) SME of (NaOCl) images surface a) PS b) Ps/PANI (0.025) ,c)PS/PANI(0.1) and cross-section d)PS , e)PS/PANI (0.025) ,f)PS/PANI(0.1).

observed that the membrane performance was changed after chlorine exposure as in Fig. 11. It was found that from 0-75 min. the FRR of PS and PS/PANI modified membranes were the same, no obvious change. After 100 min. there are two modified PS/PANI membranes (0.025- 0.1) have higher decline and 2 PS/PANI membranes have lower decline (0.2-0.4) as compared to PS membrane.

Discussion

The prepared polysulfone -polyaniline nano-composite substrate has been enhanced the performance of thin film composite as a reverse osmosis membrane. The increase in water flux is due to increase of the membrane hydro-philicity, porosity and pore size increment in addition to decreasing of the active layer thickness by adding of PANI nano-particle that increases the permeation flux [26]. These larger pores and macro-voids in the membrane

structure and more porosity made by the addition of PANI nano-particles into the casting solution facilitate water transportation through the membrane. The antifouling ability of the PS/PANI modified membranes. However, different fouling behavior indicates that the surface properties of a membrane are altered by being blended with polyaniline nano-particles. Moreover, the hydrophilic PANI nano-particle affected the surface adsorption properties of the membranes by decreasing the hydrophobic interaction between the membrane surface and BSA. Also, the presence of PANI nano-particle onto the membrane surface had a steric hindrance effect and could prevent BSA from contacting the substrate membrane [27]. These lead to a much preferable antifouling showing of the PS/ PANI nano-composite membrane than that of the PS membrane [28]. Chlorine is believed to decay polyamide macromolecules via a nucleophilic substitution reaction between chlorine and the hydrogen of the secondary amine group ($-NH$) in polyamide. The resistance of PS/PANI might be due to high chain stiffness and a high degree of cross-linking occurred. Fig. 12 shows SEM images of the membrane surfaces and their cross sections before and after exposing to sodium hypochlorite. Where; the surface of the unmodified membrane was shown to be rougher than modified membranes because of high degradation [29].

Conclusion

PANI was prepared by micellar solution method (which is not the best technique to prepare nano-composite hydrophilic PANI/PS membranes) and TFC (RO) membrane was fabricated through interfacial polymerization using a series of non-woven fabric supported PS, PS /PANI substrates, which were prepared by varying PANI contents in the casting solution ranging from 0 to 0.4 wt%. It was found that with increasing PANI content in the substrate matrix, the surface pore size, porosity and hydro-philicity of PS / PANI substrates increased. EDX and SEM confirmed the formation of Polysulfone with polyaniline nano-particle composite membranes. Water flux and salt rejection performances revealed that permeate flux was improved from 57 to 66 L/m² h, while salt rejection performances raised about 4 %. In addition, the nano-composite membrane had more resistance to organic fouling and chlorine attack.

References

1. Shannon M.A., Bohn P.W., Elimelech M., Georgiadis J.G., Mariñas B.J. and Mayes A.M., Science and technology for water purification in the coming decades, *Nature*, 452 (2008) 301-310.
2. Greenlee L.F., Lawler D.F., Freeman B.D., Marrot B. and Moulin P., Reverse osmosis desalination:

water sources, technology, and today's challenges, *Water research*, 43 (2009) 2317-2348.

3. Ali, Salah F. Abdellah, Lovert A. William, and Eman A. Fadl. "Cellulose acetate, cellulose acetate propionate and cellulose acetate butyrate membranes for water desalination applications." *Cellulose* 27.16 (2020): 9525-9543.
4. Fane A.G., Chong T.H. and Le-Clech P., Fouling in membrane processes, *Membrane Operations: Innovative Separations and Transformations*, (2009) 121-138.
5. Shen L, Huang Z, Liu Y, Li R, Xu Y, Jakaj G, Lin H. Polymeric membranes incorporated with ZnO nanoparticles for membrane fouling mitigation: A brief review. *Frontiers in chemistry*. 2020; 8.
6. Baker CO, Huang X, Nelson W, Kaner RB. Polyaniline nanofibers: broadening applications for conducting polymers. *Chemical Society Reviews*. 2017;46 (5):1510-25.
7. Shalibor, Abdolrahman, Ali Reza Modarresi-Alam, and Richard B. Kaner. "Optically active poly [2-(sec-butyl) aniline] nanofibers prepared via enantioselective polymerization." *ACS omega* 3.12 (2018): 18895-18905.
8. Fan Z., Wang Z., Sun N., Wang J. and Wang S., Performance improvement of polysulfone ultrafiltration membrane by blending with polyaniline nanofibers, *Journal of Membrane Science*, 320 (2008) 363-371.
9. Kumar, Vipin, et al. "Cationic scavenging by polyaniline: boon or bane from synthesis point of view of its nanocomposites." *Polymer* 149 (2018): 169-177.
10. Fan Z., Wang Z., Duan M., Wang J. and Wang S., Preparation and characterization of polyaniline/polysulfone nanocomposite ultrafiltration membrane, *Journal of Membrane Science*, 310 (2008) 402-408.
11. Guillen G.R., Farrell T.P., Kaner R.B. and Hoek E.M., Pore-structure, hydrophilicity, and particle filtration characteristics of polyaniline-polysulfone ultrafiltration membranes, *Journal of Materials Chemistry*, 20 (2010) 4621-4628.
12. Zhao S., Wang Z., Wei X., Zhao B., Wang J., Yang S. and Wang S., Performance improvement of polysulfone ultrafiltration membrane using PANiEB as both pore forming agent and hydrophilic modifier, *Journal of Membrane Science*, 385 (2011) 251-262.
13. Kim B. J., Oh S. G., Han M. G. and Im S. S., Preparation of polyaniline nanoparticles in micellar solutions as polymerization medium, *Langmuir*, 16 (2000) 5841-5845.
14. Asua J.M., *Polymeric dispersions: principles and applications*, Springer Science & Business Media, 2012.
15. Ali M.E., Wang L., Wang X. and Feng X., Thin film composite membranes embedded with

- graphene oxide for water desalination, *Desalination*, 386 (2016) 67-76.
16. Bandgar D., Khuspe G., Pawar R., Lee C. and Patil V., Facile and novel route for preparation of nanostructured polyaniline (PANI) thin films, *Applied Nanoscience*, 4 (2014) 27-36.
 17. Heydari, Farhood, et al. "Nanosized amorphous (Co, Fe) oxide particles decorated PANI-CNT: facile synthesis, characterization, magnetic, electromagnetic properties and their application." *International Nano Letters* 7.4 (2017): 275-283.
 18. Slimane, Amel B., Ahmed F. Al-Hossainy, and Mohamed Sh Zoromba. "Synthesis and optoelectronic properties of conductive nanostructured poly (aniline-co-o-aminophenol) thin film." *Journal of Materials Science: Materials in Electronics* 29.10 (2018): 8431-8445.
 19. Saleh T.A. and Gupta V.K., Synthesis and characterization of alumina nano-particles polyamide membrane with enhanced flux rejection performance, *Separation and purification technology*, 89 (2012) 245-251.
 20. Fathizadeh M., Aroujalian A. and Raisi A., Effect of lag time in interfacial polymerization on polyamide composite membrane with different hydrophilic sub layers, *Desalination*, 284 (2012) 32-41.
 21. Jin Y. and Su Z., Effects of polymerization conditions on hydrophilic groups in aromatic polyamide thin films, *Journal of Membrane Science*, 330 (2009) 175-179.
 22. Al-Hobaib A.S., Al-sheetan K.M., Shaik M.R., Al-Andis N.M. and Al-Suhybani M., Characterization and evaluation of reverse osmosis membranes modified with Ag₂O nanoparticles to improve performance, *Nanoscale research letters*, 10 (2015) 379.
 23. Xiao H.M., Zhang W.D., Lv C., Fu S.Y., Wan M.X. and Mai Y.W., Large enhancement in conductivity of polyaniline films by cold stretching, *Macromolecular Chemistry and Physics*, 211 (2010) 1109-1116.
 24. Hosseini S., Jeddi F., Nemati M., Madaeni S. and Moghadassi A., Electrodialysis heterogeneous anion exchange membrane modified by PANI/MWCNT composite nanoparticles: preparation, characterization and ionic transport property in desalination, *Desalination*, 341 (2014) 107-114.
 25. Mo H., Tay K.G. and Ng H.Y., Fouling of reverse osmosis membrane by protein (BSA): effects of pH, calcium, magnesium, ionic strength and temperature, *Journal of Membrane Science*, 315 (2008) 28-35.
 26. Le-Clech P., Chen V. and Fane T.A., Fouling in membrane bioreactors used in wastewater treatment, *Journal of Membrane Science*, 284 (2006) 17-53.
 27. Fan, Z., Wang, Z., Duan, M., Wang, J., & Wang, S. Preparation and characterization of polyaniline/polysulfone nanocomposite ultrafiltration membrane. *Journal of Membrane Science*, 2008, 310(1-2), 402-408.
 28. Razali N.F., Mohammad A.W. and Hilal N., Effects of polyaniline nanoparticles in polyethersulfone ultrafiltration membranes: Fouling behaviours by different types of foulant, *Journal of Industrial and Engineering Chemistry*, 20 (2014) 3134-3140.
 29. Lee W., Kang S. and Shin H., Sludge characteristics and their contribution to microfiltration in submerged membrane bioreactors, *Journal of Membrane Science*, 216 (2003) 217-227.